Lattice thermal conductivity in superlattices: molecular dynamics calculations with a heat reservoir method

2003 J. Phys.: Condens. Matter 15 8679

(http://iopscience.iop.org/0953-8984/15/50/002)

INSTITUTE OF PHYSICS PUBLISHING JOURNAL OF PHYSICS: CONDENSED MATTER

J. Phys.: Condens. Matter **15** (2003) 8679–8690 PII: S0953-8984(03)66329-0

Lattice thermal conductivity in superlattices: molecular dynamics calculations with a heat reservoir method

K Imamura[1], Y Tanaka[1], N Nishiguchi[1], S Tamura[1] and H J Maris[2]

[1] Department of Applied Physics, Hokkaido University, Sapporo 060-8628, Japan
[2] Department of Physics, Brown University, Providence, RI 02912, USA

Received 16 July 2003
Published 3 December 2003
Online at stacks.iop.org/JPhysCM/15/8679

Abstract

We report on a molecular dynamics study of the cross-plane lattice thermal conductivity in GaAs/AlAs superlattices. The layers of the superlattice are modelled by a three-dimensional face centred cubic lattice with cubic anharmonicity, and with atomic scale roughness at the interfaces. We perform the simulation of heat flow for a section of a superlattice with high- and low-temperature thermal reservoirs attached to opposite ends. The calculation reproduces qualitatively the features observed experimentally, i.e., the dramatic reduction of the conductivity relative to the conductivity of the bulk constituent materials, and the variation of the thermal conductivity with the superlattice repeat distance. The results are also in agreement with those obtained previously by Daly *et al* (2002 *Phys. Rev.* B **66** 024301) who determined the thermal conductivity from the time taken for an initially inhomogeneous temperature distribution to relax.

1. Introduction

Recently, the thermal conductivity (κ_{SL}) in dielectric and semiconducting multilayered structures, or superlattices, has been measured by several groups [1–7]. It has been found that κ_{SL} is substantially reduced relative to the conductivity of the bulk materials making up the structure. In particular, Capinski *et al* [4, 5] made measurements with GaAs/AlAs samples of various repeat distances over a wide range of temperatures (100–375 K). At 300 K, for instance, they observed that the thermal conductivity was between three and ten times less than that of bulk GaAs κ_{GaAs}, depending on the repeat distance. A similar reduction has been found in Si/Ge [6], and Bi_2Te_3/Sb_2Te_3 superlattices [7]. Control of the thermal conductivity of superlattices is important for device applications. For structures used in semiconductor lasers, a high thermal conductivity is required whereas a low thermal conductance is needed for thermoelectric applications.

0953-8984/03/508679+12$30.00

In semiconductor superlattices thermal energy is transported primarily by phonons. The kinetic formula gives the thermal conductivity κ as

$$\kappa = C\langle v^2\rangle\tau, \tag{1}$$

where C is the specific heat, $\langle v^2\rangle$ is the average of the square of the component of the phonon group velocity *in the direction of heat flow* and τ is the average phonon lifetime. It is believed that the modification of the phonon group velocity in a multilayered system [8–10] makes a significant contribution to the reduction in the thermal conductivity. This effect has been analysed by several groups [11, 12]. However, the modification of the phonon group velocity was found to not be the only factor contributing to the change in the conductivity. Since the specific heat of a superlattice is unlikely to have a significant variation with the repeat distance, the conclusion is that there must be a change in the phonon relaxation time [13–15]. However, a completely quantitative theory of the phonon relaxation time and the thermal conductivity κ_{SL} in superlattices has not yet been achieved.

As an alternative approach, Daly *et al* [16] have recently used a molecular dynamics (MD) simulation to study the thermal conductivity in superlattices. In their study, they considered an initial temperature distribution of the form

$$T(x, t = 0) = T_0 + \Delta T_0 \cos(2\pi x/L_x), \tag{2}$$

where the initial temperature perturbation ΔT_0 was 10% of the mean temperature T_0 and L_x was the length of the sample in the x-direction (the growth direction). They then used MD to determine the rate at which the amplitude $\Delta T(t)$ (with $\Delta T(0) = \Delta T_0$) of the spatial temperature variation in $T(x, t)$ was modified by heat diffusion. From the rate at which the temperature distribution relaxed, it was possible to deduce the thermal diffusion coefficient and the thermal conductivity. When calculations were performed for a model with rough interfaces, the thermal conductivity that was obtained exhibited the variation with layer thickness that had been found experimentally.

The method employed by Daly *et al* has the advantage that the thermal conductivity can be obtained with a relatively short computational time. However, an interesting problem arose in the analysis. Based on the standard equation for heat diffusion in one dimension, $\Delta T(t)$ should vary with time according to $\Delta T_0 \exp(-4\pi^2\kappa t/CL_x^2)$. However, it was found that this formula did not give a good fit to the simulated $\Delta T(t)$ for small values of t. This was connected to the fact that the heat diffusion equation has the unphysical property, i.e., an infinite spreading velocity in the limit $t \to 0$ [17]. Daly *et al* made an ad hoc modification of the solution of the diffusion equation so that for small t, the distance that heat flows is of the order of $\bar{v}t$, where $\bar{v}$ is an average phonon velocity. With this modification, it was possible to obtain a good fit to the simulated $\Delta T(t)$. So, the comparison of the results obtained by Daly *et al* with another method for the determination of the thermal conductivity which does not rely on this modification is important.

In the standard method for the simulation of thermal conductivity, the ends of the 'sample' are attached to hot and cold reservoirs and the heat flow through the sample is determined [18–24]. (For other methods, for instance relying on the density- and heat-current correlation functions, and thermal Kubo formula, see [25, 26].) Thus the purpose of the present study is to employ this heat-reservoir method of MD simulation for the lattice thermal conductivity in superlattices and see if the same results are obtained as were found by Daly *et al* when the parameters of the sample are the same. We will see that the present calculations lead to essentially the same results as obtained by Daly *et al*. In addition, we report on a number of tests that we have made to investigate the dependence of the result for the thermal conductivity on the length of the sample, i.e., L_x, and also on the transverse dimensions. These tests are important because in a finite size system some part of the energy is not transported diffusively,

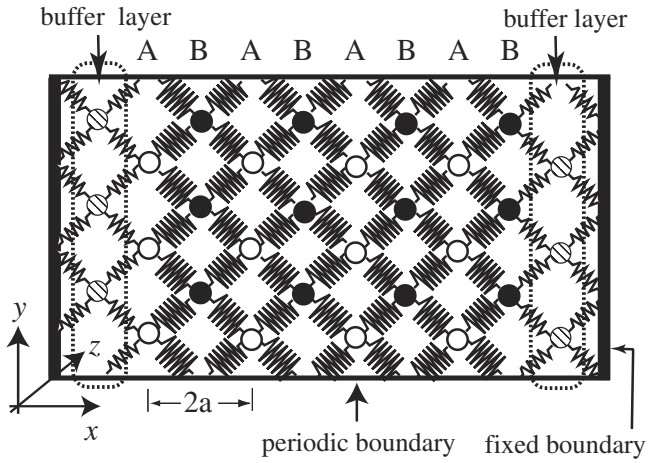

Figure 1. Schematic two-dimensional diagram of the $(GaAs)_1(AlAs)_1$ superlattice used in the MD simulations with A = GaAs (open circles) and B = AlAs (full circles). The atoms are connected by anharmonic springs between nearest neighbours. Buffer layers (hatched circles) are attached at both ends of the superlattice. The atoms in the buffer layers are connected with harmonic springs and end atoms interact directly with thermal reservoirs (which are not shown in the figure). Fixed boundaries are introduced at the both ends of the system in the longitudinal x-direction and periodic boundary conditions are assumed in the lateral (y- and z-) directions.

i.e., some phonons will be able to travel without scattering from one end of the sample to the other. Thus, to obtain a reliable result for the thermal conductivity it is necessary to simulate heat flow in a sample of sufficient size.

In section 2, we describe the basic formulation for our MD simulations. In section 3, numerical results for the thermal conductivity are presented for a GaAs/AlAs superlattice with and without disorder at the interfaces.

2. Molecular dynamics simulation

2.1. Lattice model

We consider a periodic superlattice whose unit period consists of two layers of fcc lattice (A and B), each with lattice constant a. The interface between consecutive layers lies between two adjacent (100) planes of atoms (see figure 1). The undisplaced positions of atoms are $\mathbf{r} = (n_x a, n_y a, n_z a)$, where (n_x, n_y, n_z) are integers whose sum is an even integer. In the slab A (B), atoms of mass M_A (M_B) are connected to their 12 nearest neighbours by harmonic and anharmonic springs described by a potential which is the same for A–A, B–B and A–B pairs of atoms [27].

To carry out the MD simulation, it is convenient to replace the full potential energy by an expansion to third order in the displacements of atoms from the equilibrium configuration, i.e., to write

$$\phi = -\tilde{C} + \tfrac{1}{2}\beta(r - \sqrt{2}a)^2 + \tfrac{1}{6}\beta'(r - \sqrt{2}a)^3, \tag{3}$$

where $\tilde{C}$ is a constant, r is the instantaneous distance between the atoms, and $\sqrt{2}a$ is the nearest neighbour spacing. The coefficients involved in this expression are related to measurable

quantities through

$$\beta = \frac{3\tilde{B}a}{2} \tag{4}$$

and

$$\beta' = -\frac{9\tilde{B}\gamma}{\sqrt{2}}, \tag{5}$$

where $\tilde{B}$ is the bulk modulus and γ is the Grüneisen constant [28]. We write the thickness of a slab A (B) as $d_A = n_A a$ ($d_B = n_B a$), where n_A (n_B) is the number of atomic monolayers. The length of one period is $D = d_A + d_B$. The overall dimensions of the sample are $L_x = N_x a$, $L_y = N_y a$, $L_z = N_z a$ and periodic boundary conditions to the atomic motion in the lateral directions (the y- and z-directions) are applied.

In the simulations we add 'buffer' layers consisting of a monolayer of A atoms to both ends of the superlattice. The atoms in the buffer layers are connected by harmonic springs of strength β to the superlattice atoms and also to a fixed boundary (see figure 1). The end atoms in the buffer layers exchange energies with thermal reservoirs, resulting in a heat flow through the superlattice.

We use the above structure as a model of a GaAs/AlAs superlattice and denote it as $(\mathrm{GaAs})_{n_A}(\mathrm{AlAs})_{n_B}$. Here we note that GaAs and AlAs have the zinc blende structure with two atoms in the unit cell. So in the fcc model, we assign a single GaAs (AlAs) molecule to a lattice point in the A (B) layer [12].

2.2. Parameters

We set the parameters to the same values as used by Daly *et al* [16]. Thus, $M_A = 1.20 \times 10^{-22}$ g and $M_B = 0.85 \times 10^{-22}$ g. We use the same lattice constant $a = 2.24$ Å and the same force constant $\beta = 2.56 \times 10^4$ g s^{-2} for both lattices. The Grüneisen constant is taken as $\gamma = 1$.

2.3. Thermal reservoirs and heat flux

Let the temperatures of the hot and cold reservoirs be T_H and T_L, respectively. These reservoirs interact with the atoms in the buffer layers at the ends ($n_x = 0$ and $N_x + 1$) of the superlattice [18, 20]. The interaction amounts to changing the energy of an atom in the buffer layer at the hot end to a new random value which is chosen from a Maxwell–Boltzmann distribution corresponding to the temperature T_H. The direction of motion of the atom after this interaction is random. Energy exchange with the cold reservoir is handled in a similar way. The unit time step in the simulation is 4.4 fs and the interaction is assumed to occur every 20 time steps, so energy exchange with the buffer layer occurs every $\delta t = 88$ fs. This value has been chosen because the thermal boundary resistance (Kapitza resistance) between the heat reservoirs and the superlattice is minimized for δt in the vicinity of this value. We discuss this Kapitza resistance in more detail in section 3.1 below.

We write the heat flux flowing (normal to the superlattice interfaces) from the hot reservoir into the superlattice as $j_H(t)$ and that flowing into the cold reservoir from the superlattice as $j_L(t)$. To reduce the fluctuation in time of the calculated $j_{H,L}(t)$, we take averages of the heat flux over an appropriate time interval Δt

$$\langle j_{H,L}(t)\rangle = \frac{1}{\Delta t}\int_{t-\Delta t/2}^{t+\Delta t/2} j_{H,L}(t')\,\mathrm{d}t'. \tag{6}$$

Figure 2 shows the averaged heat flux $\langle j_H(t)\rangle$ flowing out from the hot reservoir and $\langle j_L(t)\rangle$ flowing into the cold reservoir for a $(\mathrm{GaAs})_1(\mathrm{AlAs})_1$ superlattice. In this calculation we have

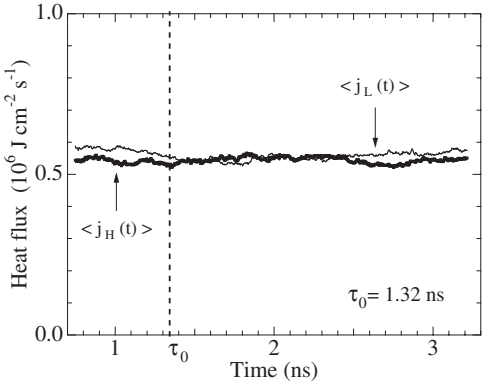

Figure 2. Heat flux flowing into ($\langle j_{\rm H}\rangle$, bold curve) and flowing out of ($\langle j_{\rm L}\rangle$, thin curve) the $(GaAs)_1(AlAs)_1$ superlattice. For time after τ_0, the superlattice is in a state in which there is a steady heat flow.

taken $\Delta t = 1.5$ ns ($=3.4 \times 10^5$ time steps). After a time τ_0 of around 1.32 ns from the beginning of the simulation, the fluxes $\langle j_{\rm H}(t)\rangle$ and $\langle j_{\rm L}(t)\rangle$ become almost identical, and a steady heat flow exists inside the superlattice.

2.4. Temperature gradient

The local temperature $T(x)$ in the superlattice as a function of the longitudinal coordinate x is defined by taking the average of the kinetic energy of all molecules in the cross sectional area (in the y–z plane) and then taking an average over time

$$T(x = n_x a) = \frac{4}{3k_{\rm B}N_yN_z}\sum_{n_y,n_z}\frac{\langle p^2_{(n_x,n_y,n_z)}\rangle_t}{2M_{n_x}}, \tag{7}$$

where $\langle\cdots\rangle_t$ means the time average in the steady state ($t > \tau_0$) and M_{n_x} is either $M_{\rm A}$ or $M_{\rm B}$ depending on the position $x = n_x a$. It should be noted that the total number of lattice points in the y–z plane is $N_yN_z/2$ for the fcc lattice we consider. This brings the extra factor 2 in the numerator of equation (7). Once the heat current $J_x(=j_{\rm H} = j_{\rm L})$ and the temperature distribution $T(x)$ are determined, the thermal conductivity κ can be calculated from Fourier's law

$$J_x = -\kappa\nabla_x T(x). \tag{8}$$

3. Results

3.1. Temperature profiles

Figure 3(a) illustrates the calculated temperature profile of the $(GaAs)_1(AlAs)_1$ superlattice (without any disorder). The temperatures of the reservoirs are $T_{\rm H} = 330$ K and $T_{\rm L} = 270$ K. It can be seen that the temperature varies linearly with distance, and that the temperatures $T'_{\rm H}$ and $T'_{\rm L}$ at the ends of the superlattice differ appreciably from the reservoir temperatures. This is a result of the Kapitza resistance which is dependent on the nature of the coupling of the superlattice with the reservoirs. The ideal reservoir would be a perfect emitter and absorber of phonons of all frequencies and polarizations and so would have no Kapitza resistance. But it does not appear simple to create such a reservoir. For fixed values of $T_{\rm H}$ and $T_{\rm L}$ the

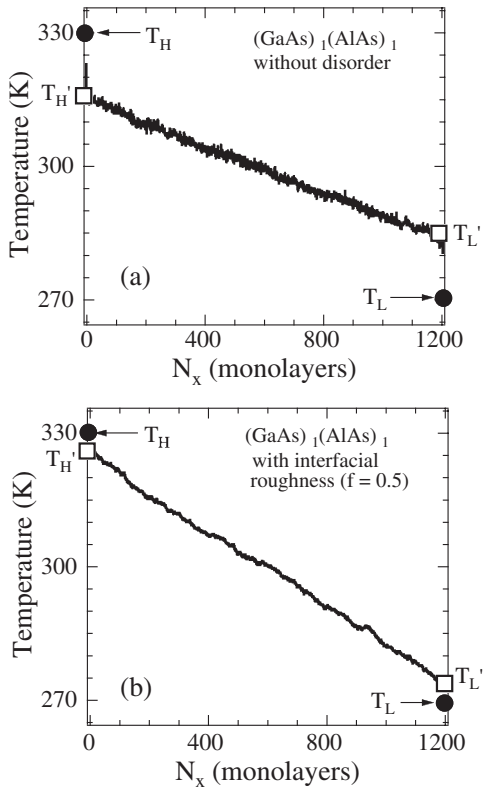

Figure 3. Temperature profiles in the superlattice in the steady state. $T_{\mathrm{H}} = 330$ K and $T_{\mathrm{L}} = 270$ K are the temperatures at the hot and cold thermal reservoirs. (a) $(\mathrm{GaAs})_1(\mathrm{AlAs})_1$ superlattice with ideal interfaces. $T'_{\mathrm{H}} = 316$ K and $T'_{\mathrm{L}} = 284$ K are the temperatures of the end molecules in the superlattice. (b) $(\mathrm{GaAs})_1(\mathrm{AlAs})_1$ superlattice with interfacial roughness $f = 0.5$. $T'_{\mathrm{H}} = 326$ K and $T'_{\mathrm{L}} = 274$ K are the temperatures of the end molecules in the superlattice.

temperature differences $T_{\mathrm{H}} - T'_{\mathrm{H}}$ and $T'_{\mathrm{L}} - T_{\mathrm{L}}$ are smaller for a poor conductor because then there is a smaller heat flow. As an example, we show in figure 3(b) results for a superlattice of the same geometry but with interfacial roughness. Fortunately, the existence of the Kapitza resistance does not influence the size dependence and the magnitude of the thermal conductivity as we will discuss below.

Here we comment on the temperature profiles we obtained in the course of simulations. Although the temperature in the superlattice shown in figure 3 appears to vary linearly with distance, careful examination shows that there is some nonlinearity. We find that if no disorder is present, the temperature decreases exponentially rather than linearly on going from the hot to the cold end. This can be more easily seen if a larger temperature difference $T_{\mathrm{H}} - T_{\mathrm{L}}$ is assumed (figure 4(a)). The heat flux is the same throughout the superlattice, and so from Fourier's law the product of κ with $\mathrm{d}T/\mathrm{d}x$ must be constant. Consequently, an exponential profile indicates that the thermal conductivity varies as T^{-1}. This is the situation for ordered systems where anharmonicity resists the heat flow. In this case the phonons scatter only off phonons and so the scattering rate goes as T, and the conductivity goes as the inverse of temperature.

However, when there exists disorder, such as interfacial roughness for short-period superlattices, the temperature in the superlattices no longer varies exponentially with distance,

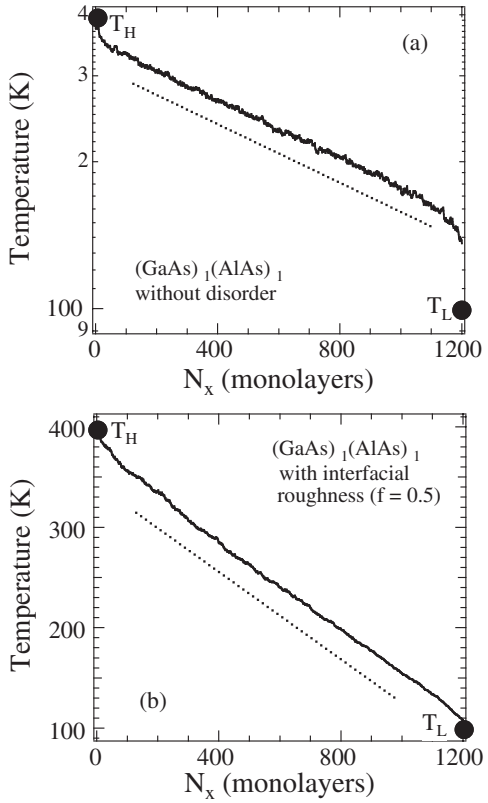

Figure 4. Temperature profiles for $T_H = 400$ K and $T_L = 100$ K. (a) $(GaAs)_1(AlAs)_1$ superlattice with ideal interfaces and (b) $(GaAs)_1(AlAs)_1$ superlattice with interfacial roughness $f = 0.5$. Note the log- and linear-scale for the vertical axis of (a) and (b), respectively. The dotted straight lines are guides to the eye.

but instead varies closer to linearly in distance (figure 4(b)). If we have a linear temperature profile, the conductivity deduced from Fourier's law should be independent of temperature. This is in accord with the fact that the scattering from the disorder is temperature independent and this leads to the conductivity being independent of temperature.

We note, however, that the temperature profile which we approximate as linear in distance for ideal superlattices (without any disorder) does not affect the magnitudes of the thermal conductivity in the present simulations.

3.2. Size dependence of the thermal conductivity

In determining the thermal conductivity from the simulations, we have to pay attention to the fact that when Fourier's law holds, the thermal conductivity should be independent of the system size. However, if the size of the superlattice assumed in the simulations is small, some of the phonons travel ballistically over the distance between the reservoirs. The presence of these unscattered phonons leads to a thermal conductivity depending on the system size. In order to avoid this situation, we have first determined the appropriate dimension of the system from the simulations for bulk GaAs.

Figure 5 exhibits the dependence of the calculated bulk thermal conductivity κ_{GaAs} on the sample length N_x. For $N_x > 1200$, the thermal conductivity becomes fairly insensitive

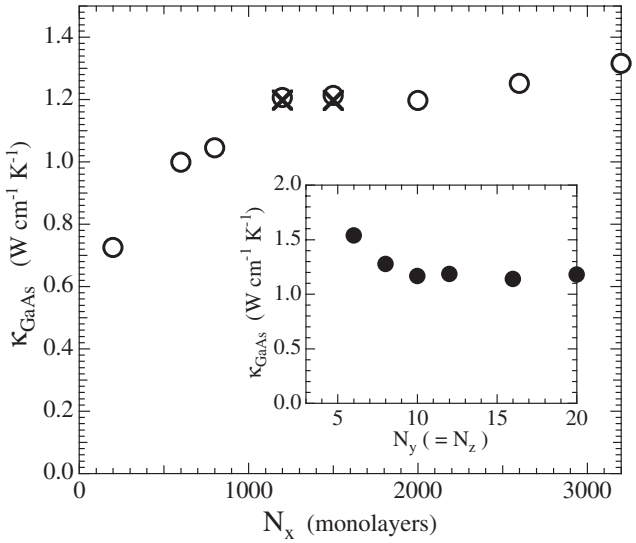

Figure 5. Size dependence of the simulated thermal conductivity κ_{GaAs} in bulk GaAs. κ_{GaAs} versus longitudinal lattice length $L_x = N_x a$ for $N_y = N_z = 12$ is shown by open circles for $T_{\mathrm{H}} = 330$ K and $T_{\mathrm{L}} = 270$ K. Crosses are the same κ_{GaAs} for $T_{\mathrm{H}} = 390$ K and $T_{\mathrm{L}} = 210$ K. In each case, the central temperature is $T = 300$ K. Inset illustrates κ_{GaAs} versus lateral lattice dimension $L_y = L_z = N_y a$ for $N_x = 1200$ at $T_{\mathrm{H}} = 330$ K and $T_{\mathrm{L}} = 270$ K.

to the system size. Also, we show in the same figure the dependence of κ_{GaAs} on lateral size. We find that for $N_y = N_z > 10$, the thermal conductivity depends only weakly on the lateral dimensions. A similar lateral size dependence of thermal conductivity has been found by Schelling *et al* [24] and also by Daily *et al* [16]. A moderate dependence of the thermal conductivity on lateral dimensions was discussed in some detail by Schelling *et al*. However, we have not attempted to make a detailed comparison of our results with their ideas.

These results are obtained by taking the temperatures of the reservoirs as $T_{\mathrm{H}} = 330$ K and $T_{\mathrm{L}} = 270$ K. We have also changed the temperatures of the reservoirs to $T_{\mathrm{H}} = 390$ K and $T_{\mathrm{L}} = 210$ K and calculated κ_{GaAs} for $N_x = 1200$ and 1500. The results are also shown in figure 5 with crosses. To within the uncertainty, we find the same magnitudes for κ_{GaAs}, implying that the thermal conductivity is insensitive to the temperatures of the reservoirs assumed.

Although a larger size for the system is expected to give a more accurate result, it is time consuming. As the length increases, the time increases not only because there are more atoms, but also because a longer time is needed before steady state is achieved. In most of the simulations, we therefore study superlattices of size $N_x = 1200$, $N_y = 12$, and $N_z = 12$. The simulations were performed on a Hitachi SR8000 supercomputer and took CPU times up to 6 h for bulk GaAs and 8 h for a $(\mathrm{GaAs})_1(\mathrm{AlAs})_1$ superlattice with rough interfaces. This sample size should be compared with $N_x = 3200$, $N_y = 20$, $N_z = 20$ used by Daly *et al* in their study [16]. Daly *et al* calculated the thermal conductivity by simulating the diffusion of heat with an initial temperature profile they set up in the system, whereas in our simulations the data available for deducing the thermal conductivity are acquired only after the system becomes stationary. For this reason, the present simulations take a greater computation time, and to compensate for this we have to use a smaller sample than was used by Daly *et al*.

The absolute value of the thermal conductivity in bulk GaAs obtained from the present simulation with the parameters as given above is $\kappa_{\mathrm{GaAs}} = 1.21$ W cm^{-1} K^{-1} at 300 K. This is

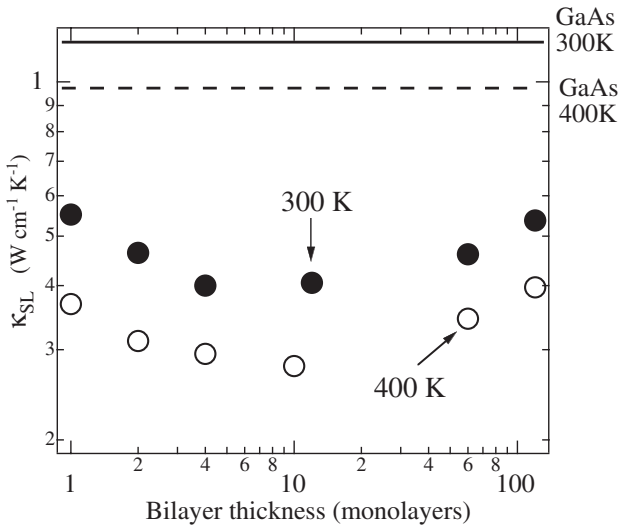

Figure 6. The simulated thermal conductivity κ_{SL} for ideal superlattices versus the number of bilayers. The full circles and open circles represent the thermal conductivity at 300 and 400 K, respectively. The system size assumed is $N_x = 1200$, $N_y = 12$ and $N_z = 12$. The solid and dashed lines represent the thermal conductivity κ_{GaAs} calculated from simulations of bulk GaAs at the two temperatures.

close to the value 0.99 W cm^{-1} K^{-1} [16] obtained by Daly *et al* at the same temperature but about a factor of 2–3 larger than the experimental value $\kappa^{expt}_{GaAs} = 0.45$ W cm^{-1} K^{-1} [5]. This discrepancy is not surprising because our lattice model is much simpler than the real structure, and the simulated κ_{GaAs} depends crucially on the assumed value of the Grüneisen parameter. Moreover, the disorder due to mass defects and so on is not included.

3.3. Superlattice with ideal interfaces

Figure 6 shows the calculated thermal conductivity κ_{SL} versus repeat distance in GaAs/AlAs superlattices (at 300 and 400 K) with ideal interfaces together with the bulk thermal conductivity κ_{GaAs}. For all bilayer thickness κ_{SL} at 400 K is smaller than at 300 K and their relative magnitude is in accord with the value expected from T^{-1}-law of the thermal conductivity.

For short period superlattices the calculation gives a reduction factor that increases as the period becomes longer. More precisely, we see that the calculated κ_{SL} decreases monotonically as the layer thickness increases and at $n_A = n_B \equiv \tilde{n} = 10$ approaches a value of about $1/3$ of the bulk κ_{GaAs}. This behaviour has not been observed experimentally (see figure 7) but is in agreement with the previously reported reduction of the thermal conductivity (displayed in the same figure 7) [12] due to the zone-folding effect. The opening of frequency gaps at the mini-Brillouin zone centre and boundaries lowers the average phonon group velocity. Thus, our calculation supports the hypothesis that the zone-folding is the dominant effect on the thermal conductivity in the short period superlattices without disorder.

In contrast, for the longer period superlattices the simulation indicates that κ_{SL} begins to increase slowly, as is seen in the experimental data. Thus the simulated thermal conductivity in GaAs/AlAs superlattices with ideal interfaces can only explain the experimental results for long period superlattices. Apart from the overall magnitude of a factor of 20%, all these results for perfect superlattices shown in figure 6 are in good agreement with the simulated results of Daly *et al* for the entire region of bilayer thickness plotted.

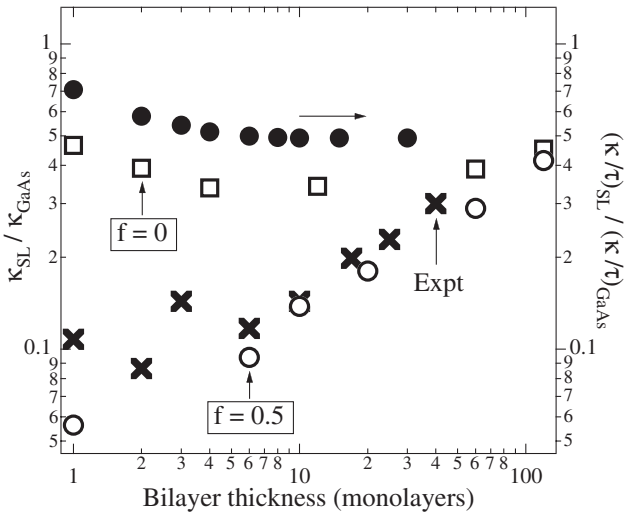

Figure 7. Comparison of the simulated thermal conductivity κ_{SL} (normalized by κ_{GaAs}) between an ideal superlattice $f = 0$ (squares) and a rough superlattice $f = 0.5$ (open circles) together with the experimental results (crosses) from [5]. The experimental error is approximately 10%. Full circles are the results obtained with only the effect of group velocity reduction due to zone-folding effects (from [12]) (τ in the vertical axis is the average phonon relaxation time). The system size is $N_x = 1200$, $N_y = 12$, $N_z = 12$. The temperature is 300 K.

Here we note that the existence of a minimum thermal conductivity at a certain repeat distance and the subsequent increase of the thermal conductivity qualitatively coincide with the experiment by Venkatasubramanian with Bi_2Te_3/Sb_2Te_3 superlattices [7], where the minimum thermal conductivity has been observed for a period of 50 Å. A possible explanation for the existence of the conductivity minimum based on the idea of the crossover between the particle and wave nature for phonons has been given by Gurzhi *et al* [29], and Simkin and Mahan [30].

It is tempting to make an analogy between the minimum thermal conductivity found here and the well-known Knudsen minimum that occurs for the flow of gas along a tube. However, as pointed out by Simkin and Mahan [30] the minimum in the heat flow in superlattices is related to the cross-over between particle and wave-interference transport, whereas the Knudsen minimum in gas flow is an effect that can be understood entirely within a theory based on the Boltzmann equation [31].

3.4. Superlattices with interfacial roughness

A transition region containing both layer constituents exists typically at the boundary between adjacent layers, usually with a thickness of about a monolayer [5, 32]. In order to calculate the effects of this interfacial roughness on the heat flow in superlattices, we use the same model assumed by Daly *et al* [16]. Explicitly, for the last atomic monolayer of each superlattice layer, the mass of each atom is randomly assigned to be the mass of a GaAs molecule or an AlAs molecule, with a probability given by the roughness factor f (thus, f varies in the range between 0 and 0.5).

The results of simulations performed for rough superlattices with $f = 0.5$ at 300 K are shown in figure 7, along with the results for the ideal superlattices with $f = 0$ and the experimental data. The results indicate that the introduction of the roughness at the interfaces dramatically reduces the thermal conductivity of the shortest period superlattices.

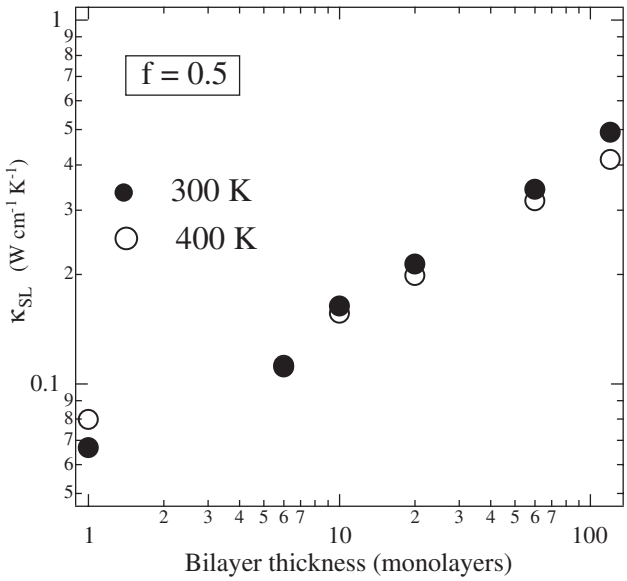

Figure 8. Thermal conductivity versus number of bilayers for rough superlattices. The full (open) circles represent the calculated values at 300 K (400 K).

This reduction is by almost an order of magnitude for $f = 0.5$. As expected, the effect decreases with increasing superlattice period, and for the $(GaAs)_{120}(AlAs)_{120}$ superlattice we find no significant effect on the thermal conductivity. The thermal conductivity of these rough superlattices increases with increasing bilayer thickness over the entire range of periods. This sort of behaviour is what has already been seen in the simulations by Daly *et al*, as well as in experiments. Specifically, the overall magnitude of the normalized thermal conductivity $\kappa_{SL}/\kappa_{GaAs}$ coincides well with the experimentally measured thermal conductivity except for $\tilde{n} < 5$, where some fluctuations are observed in the experiments. Thus, it appears that interfacial roughness may account for the discrepancy between the calculated reduction in the thermal conductivity in the superlattices without disorder and the reduction observed in the experimental data.

The thermal conductivity of the superlattices with a roughness factor $f = 0.5$ is compared in figure 8 for 300 and 400 K. In distinction to the case for the superlattices with ideal interfaces (figure 6), we find no significant change in κ_{SL} at these temperatures. This is the result that is expected if the interfacial thermal resistance becomes the dominant effect which prevents the heat conduction in superlattices.

4. Conclusion

In the present work we have calculated the lattice thermal conductivity κ_{SL} in GaAs/AlAs superlattices in the growth direction based on a conventional MD simulation which assumes hot and cold thermal reservoirs at opposite ends of the superlattice sample. Our results are found to be in good agreement with those of Daly *et al* who employed a different MD calculation for the same problem. This agreement gives support to the method used by Daly *et al* to obtain the thermal conductivity from the rate of decay of an inhomogeneous temperature distribution.

The MD calculations have proven to be a powerful method for studying the thermal conductivity in superlattices. In future work, we plan to apply the MD approach to the study of heat conduction in disordered crystals and glasses with structural disorder.

Acknowledgments

This work was supported in part by a Grant-in-Aid for Scientific Research from the Ministry of Education, Culture, Sports, Science and Technology (MEXT) of Japan (Grant Number 12640304), by a Grant-in-Aid for JSPS Fellows from the MEXT of Japan, and by the US Air Force Office of Scientific Research MURI grant entitled 'Phonon Enhancement of Electronic and Optoelectronic Devices,' (Grant No. F4962-00-1-0331).

References

[1] Yao T 1987 *Appl. Phys. Lett.* **51** 1798
[2] Weilert M A, Msall M A, Anderson A C and Wolfe J P 1993 *Phys. Rev. Lett.* **71** 735
Weilert M A, Msall M A, Anderson A C and Wolfe J P 1993 *Z. Phys.* B **91** 179
[3] Chen G, Tien C L, Wu X and Smith J S 1994 *J. Heat Transfer* **116** 325
[4] Capinski W S and Maris H J 1996 *Physica* B **219/220** 699
[5] Capinski W S, Cardona M, Katzer D S, Maris H J, Ploog K and Ruf T 1999 *Physica* B **263/264** 530
Capinski W S, Maris H J, Ruf T, Cardona M, Ploog K and Katzer D S 1999 *Phys. Rev.* B **59** 8105
[6] Lee S M, Cahill D G and Venkatasubramanian R 1997 *Appl. Phys. Lett.* **70** 2957
[7] Venkatasubramanian R 2000 *Phys. Rev.* B **61** 3091
[8] Tamura S, Hurley D C and Wolfe J P 1988 *Phys. Rev.* B **38** 1427
[9] Tanaka Y, Narita M and Tamura S 1998 *J. Phys.: Condens. Matter* **10** 8787
Narita M, Tanaka Y and Tamura S 2002 *J. Phys.: Condens. Matter* **14** 1709
[10] Imamura K, Tanaka Y and Tamura S 2002 *Phys. Rev.* B **65** 174301
[11] Hyldgaard P and Mahan G D 1997 *Phys. Rev.* B **56** 10754
[12] Tamura S, Tanaka Y and Maris H J 1999 *Phys. Rev.* B **60** 2627
[13] Tamura S 1997 *Phys. Rev.* B **56** 12440
[14] Ren S Y and Dow J D 1982 *Phys. Rev.* B **25** 3750
[15] Schmitt M, Mayer A P and Strauch D 1999 *Physica* B **263/264** 486
[16] Daly B C, Maris H J, Imamura K and Tamura S 2002 *Phys. Rev.* B **66** 024301
[17] Simons S 1972 *Transport Theory and Statistical Physics* **2** 117
[18] Payton D N, Rich M and Visscher W M 1967 *Phys. Rev.* **160** 706
[19] Mountain R D and McDonald R A 1983 *Phys. Rev.* B **28** 3022
[20] Nishiguchi N and Sakuma T 1994 *J. Phys.: Condens. Matter* **6** 3013
[21] Hatano T 1999 *Phys. Rev.* E **59** 1
[22] Oligschleger C and Schön J C 1999 *Phys. Rev.* B **59** 4125
[23] Jund P and Jullien R 1999 *Phys. Rev.* B **59** 13707
[24] Schelling P K, Phillpot S R and Keblinski P 2002 *Phys. Rev.* B **65** 144306
[25] Ladd A J C, Moran B and Hoover W G 1986 *Phys. Rev.* B **34** 5058
[26] Allen P B and Feldman J L 1993 *Phys. Rev.* B **48** 12581
Feldman J L, Kluge M D, Allen P B and Wooten F 1993 *Phys. Rev.* B **48** 12589
[27] Maradudin A A, Flynn P A and Coldwell-Horsfall R A 1961 *Ann. Phys.* **15** 360
[28] Maris H J and Tamura S 1993 *Phys. Rev.* B **47** 727
Tamura S and Maris H J 1995 *Phys. Rev.* B **51** 2857
[29] Gurzhi R N, Il'evskii V I and Makimov A O 1975 *Fiz. Nizkikh Temp.* **1** 1330
Gurzhi R N, Il'evskii V I and Makimov A O 1975 *Sov. J. Low Temp. Phys.* **1** 638 (Engl. Transl.)
[30] Simkin M V and Mahan G D 2000 *Phys. Rev. Lett.* **84** 927
[31] Benin D and Maris H J 1978 *Phys. Rev.* B **18** 3112
[32] Ruf T, Spitzer J, Sapega V F, Belitsky V I, Cardona M and Ploog K 1994 *Phys. Rev.* B **50** 1792